Publ. Astron. Soc. Japan **40**, 511-532 (1988)

CO Observations of the Central Region of the Spiral Galaxy NGC 6946*

Yoshiaki SOFUE, Mamoru DOI, and Sumio ISHIZUKI

Institute of Astronomy, Faculty of Science, The University of Tokyo, Mitaka, Tokyo 181

and

Naomasa NAKAI and Toshihiro HANDA

Nobeyama Raido Observatory, Minamimaki-mura, Minamisaku-gun, Nagano 384-13

(Received 1988 January 29; accepted 1988 June 15)

Abstract

The central region of the Sc galaxy NGC 6946 has been observed in the ^{12}CO (J=1–0) line emission using the Nobeyama 45-m telescope with a resolution of 17″ (0.8 kpc). A high concentration of CO gas is found in the central 2 kpc with a slight elongation in the north-south direction. The global intensity distribution in the central 2-kpc radius is expressed by an exponential law of scale radius 0.9 kpc. We identify this part as the nuclear disk, while the outer main disk has an exponential distribution of scale radius 4.6 kpc. The blue-light intensity in the central 2 kpc was found to be correlated with the CO intensity as $I_{\rm blue} \propto I_{\rm CO}^{0.3}$. This fact may indicate either extremely high obscuration of star light by dense dark clouds, or a significantly lower star formation rate in the central region compared with that in the outer disk. The latter is consistent with the rapid accretion of gas toward the center and suggests a pre-starburst phase at a near nucleus. On the other hand the radio continuum intensity is shown to have a higher-power relation, $I_{\rm cont} \propto I_{\rm CO}^{2.5}$, which indicates high excitation of magnetic fields and intense acceleration of cosmic rays in the nuclear disk. The rotation curve is flat with $V_{\rm rot} \approx 200$ km s^{-1} even in the central region as close as $r \approx 500$ pc to 2 kpc, while it has a steep gradient in the central few hundred parsecs. A large noncircular motion is found and is reasonably interpreted by an inflow of 40 km s^{-1}, and the velocity field is well reproduced by a shocked-gas model in a barred potential.

Key words: Barred potential; Carbon monoxide; Galaxies; Molecular gas; Nuclear disks.

* Based on observations made at the Nobeyama Radio Observatory (NRO). NRO is a branch of the National Astronomical Observatory, an inter-university research institute operated by the Ministry of Education, Science, and Culture.

1. Introduction

NGC 6946, classified as an ScI (or II) spiral galaxy (van den Bergh 1960; Sandage and Tammann 1974, 1981), has a"heavy" optical arm on the northeastern side, which led Arp (1966) to include this galaxy in his *Atlas of Peculiar Galaxies*. Photographic and photometric observations have shown that this galaxy is a first-class luminous galaxy indicating a high rate of star formation (Hodge 1969; Ables 1971; Elmegreen and Elmegreen 1984; Beckman et al. 1986). From their Hα emission observations Beckman et al. (1986) have derived velocity curves in the central region of the galaxy and showed that there exists a radial motion superposed on the circular rotation. Lebofsky and Rieke (1979) observed this galaxy in the infrared emission at 2.2 μm and 10 μm. Their 2.2-μm map of the nuclear region shows that the nucleus is so heavily obscured that the true location of the nucleus cannot be determined from optical data.

At radio wavelengths, numerous continuum and line observations have been made. Radio continuum emission was observed at 6, 21, and 49 cm by van der Kruit et al. (1977) and at 2.8 cm by Klein et al. (1982), from which they obtained thermal and nonthermal radio distributions. From observations of the linear polarization, Klein et al. (1982) showed that both the average strength of the uniform magnetic field and the average density of the thermal electrons in NGC 6946 are several times higher than that in nearby galaxies. Gioia and Fabbiano (1987) obtained high-resolution maps at 6 and 20 cm with the VLA.

Rogstad and Shostak (1972), and Rogstad et al. (1973) (hereafter referred to as RS 1972 and RSR 1973, respectively) measured the distribution of neutral hydrogen with an angular resolution of 2′ and showed a central depression in the H I gas. Tacconi and Young (1986) mapped the H I emission with a higher resolution of about 40″. They compared the H I data with radial distributions of the CO (H_2 gas) intensity, blue luminosity, continuum, and *I*-band emission, and inferred that the formation efficiency of molecular clouds decreases with the radius.

Molecular gas plays an important role in star formation. CO observations are particularly important to study the inner disk, where most of the neutral gas is in the form of molecules, while H I gas is observed to have depression there. The first mapping of NGC 6946 in the ^{12}CO (λ=2.6 mm) line emission was made by Morris and Lo (1978) using the NRAO 11-m telescope with an angular resolution 65″. This mapping covered the northeastern quadrant of the galaxy within about 4′ from the nucleus or within 12 kpc at the distance of 10.1 Mpc (RSR 1973). They evaluated the total mass of molecular gas in the quadrant to be $3.7\times10^9\,M_\odot$, which is twice that of our Galaxy. Using the same telescope, Rickard and Palmer (1981) mapped the ^{12}CO emission in the inner disk of $3'\times3'$, where the CO intensity showed a strong concentration on the nucleus. Young and Scoville (1982) obtained the radial distribution of molecular gas from ^{12}CO (J=1–0) observations made along the major and minor axes with the FCRAO 14-m telescope (beam size $\approx$50″). The radial distribution shows a smooth decrease toward the outer disk, and is similar to the blue intensity distribution. They showed that the CO intensity is well fitted by an exponential-law distribution. Young and Sanders (1986) have also measured the ratio

of the ^{13}CO to ^{12}CO intensities across the galactic disk.

To obtain the distribution and dynamics of the molecular gas in the nuclear region, a higher spatial resolution is required. A map of CO emission with a synthesized beam of 7".6 has been made by Ball et al. (1985) with the Owens Valley Millimeter Wave Interferometer. They found a bar-like structure at position angle 160° in the velocity range of $V_{LSR}=-1.6$ to 81.6 km s^{-1}. Weliachew et al. (1988) have used the IRAM 30-m telescope to map the central 1′ in the CO line emission (HPBW=23″). They showed that the molecular gas distribution has an oval structure.

In order to investigate the precise distribution and dynamics of the molecular gas in the central region, we made new observations of the ^{12}CO ($J=1$–0) line emission using the Nobeyama 45-m filled-aperture telescope with a high angular resolution (17″) and full velocity coverage (650 km s^{-1}). We here present the results and discuss the dynamics of the gas and star formation in the nuclear disk of NGC 6946.

2. Observations and Results

(a) Observations

The observations were made in May 1985 and May 1986 using the 45-m telescope of the Nobeyama Radio Observatory (NRO). The full half-power beam width (HPBW) at the ^{12}CO ($J=1$–0) frequency of 115.271204 GHz was 17″, which corresponds to 0.83 kpc at a distance of 10.1 Mpc. Here we adopt the distance after RS 1972 and RSR 1973, so that our data can be directly compared with the recent H I and CO observations, whereas Sandage and Tammann (1981) gave a distance of 10.5 Mpc. The aperture and main beam efficiencies were 0.26 and 0.45, respectively. The receiver frontend was a cooled Schottky barrier diode mixer receiver. The system noise temperature (SSB) including the atmospheric effect and the antenna ohmic loss was 900–1500 K at the observing elevation. The spectra were taken with a 2048-channel, wide-band acousto-optical spectrometer (AOS). The instantaneous bandwidth was 250 MHz which provided velocity coverage of 650 km s^{-1}. The frequency resolution was 250 kHz corresponding to the velocity resolution of 0.65 km s^{-1}. The

Table 1. Adopted parameters for NGC 6946.

Position of the nucleus[a]	
(coordinates of the map center $X=0$, $Y=0$)	$\alpha(1950)=20^h33^m49^s.16$ (48^s.8)*
	$\delta(1950)=59°58'49''.4$ (50″.2)*
Position angle of the major axis[b]	62°
Inclination[b]	30°
Distance[b]	10.1 Mpc
V_{sys}: Systemic velocity with respect to LSR[c]	60 km s^{-1}

[a] Condon et al. 1982.
[b] RS 1972, RSR 1973.
[c] This paper.
* The coordinates of the map center ($X=0$, $Y=0$) as given in the parentheses were shifted by 3″ from the 1.5-GHz continuum peak position given by Condon et al. (1982), because we adopted more accurate coordinates of the pointing calibrator, OH 104.9+2.5, after we finished the observations during which older coordinates were used.

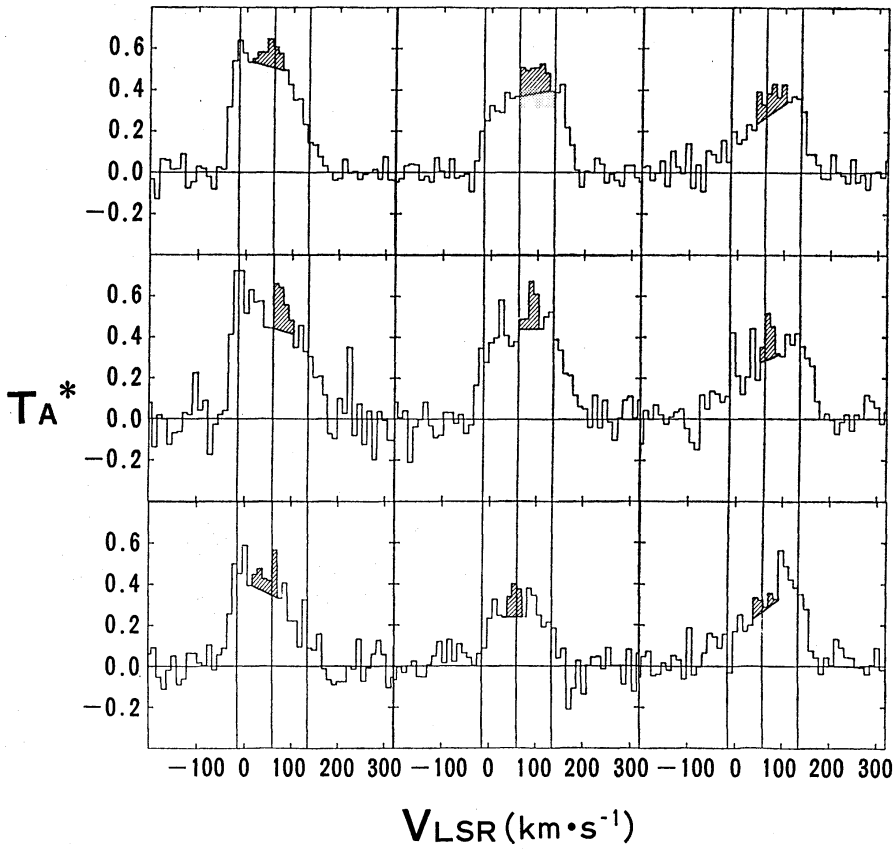

Fig. 1a. CO spectra for the central nine points. The vertical lines show $V_{LSR}=-10$, 60 (systemic velocity), and 130 km s^{-1}, respectively. The hatched part shows the enhancement at $V \approx V_{sys}$.

parameters for the observations are summarized in table 1.

The observations were made in the position switching mode. In one cycle of switching observations, one "off" position was observed after observing two or three different "on" positions. At each position the signal was integrated for 20 s in every cycle, and 15 to 30 cycles were repeated. The "off" position was adopted at 10′ east and west of the mapping center alternately. The pointing of the antenna was calibrated every 1–1.5 hr by observing a nearby SiO maser source, OH 104.9+2.4. The absolute pointing accuracy was estimated to be better than $\pm 4''$ (peak value). The calibration of the line intensity was made by using an absorbing chopper at room temperature in front of the receiver. The intensity scale used in this paper is the antenna temperature, T_A^*, corrected for the atmospheric and antenna ohmic losses but not for the beam efficiency.

(b) Line Profiles

We observed 71 points in the nuclear region of the galaxy within a $1'.5 \times 1'.5$ squares. Figure 1 shows the individual profiles. The antenna temperature T_A^* is as high as 0.6 K near the center. The filling factor of CO molecular clouds is calculated

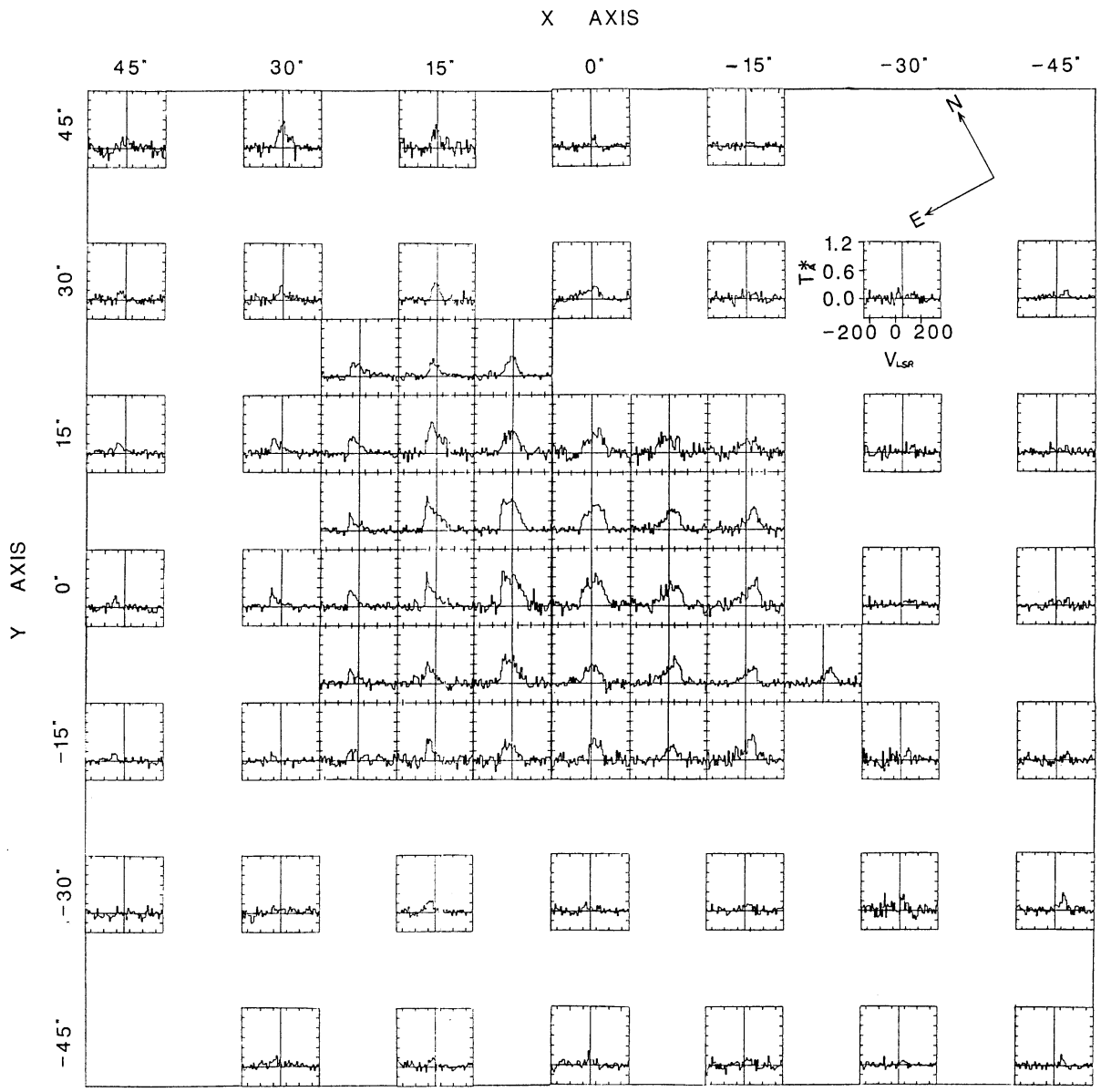

Fig. 1b. The CO spectra for the observed 71 points. The vertical line shows the systemic velocity $V_{sys} \sim 60$ km s^{-1}.

as

$$f_s \sim T_A^*/[(T_{ex}-T_{bg})\eta] \approx 0.6\ \mathrm{K}/[(36\ \mathrm{K}-3\ \mathrm{K})\times 0.45] \sim 0.11\ , \qquad (1)$$

where T_{ex} is the excitation temperature, which is assumed to be nearly the same as the dust temperature and was derived from infrared observations (Rickard and Harvey 1984), T_{bg} is the cosmic blackbody temperature, and η is the main beam efficiency. This evaluation is valid in the case where the optical depth of each molecular cloud is large enough compared to unity. This condition is shown to be satisfied in NGC 6946, because the ratio of the brightness temperatures of the $J=2$–1 and $J=1$–0 transition lines has been measured to be close to unity (Lo et al. 1980).

The CO line profiles around the center at $-7''.5<X<7''.5$, $-7''.5<Y<7''.5$ are characterized by three peaks: The peaks around $V=0$ km s^{-1} for $X>0$ and those at 130 km s^{-1} for $X<0$ are due to the contribution of the gas in the galactic rotation. In addition to these two peaks attributable to the rotation we can see another component which peaks at $V \approx V_{sys}=60$ km s^{-1}. This component is likely to be a contribution from the central singular concentration which is seen within a finite (17″) beam size (see subsection 3d).

3. Intensity Distribution

(a) Oval Distribution of the CO Emission

Figure 2 shows the distribution of the integrated CO intensity. A strong peak is found near the center. The overall distribution is slightly elongated in the north-south direction or at 30° from the minor axis. The oval distribution has been also reported by Weliachew et al. (1988). The CO distribution roughly coincides with the optical emission (6500 Å) distribution in continuum (see subsection 3e).

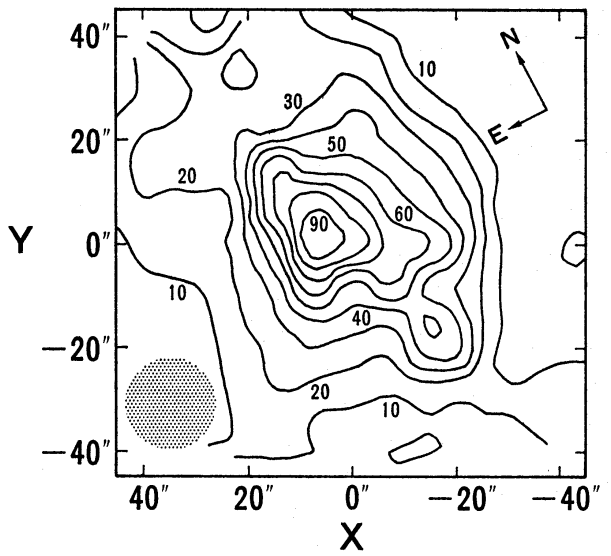

Fig. 2. Map of the integrated intensity of CO emission $I=\int T_A^*\, dv$ in K km s^{-1}. The beam size (HPBW) is indicated by the shaded circle in the lower left corner.

Ball et al. (1985) reported detection of a molecular bar at position angle of $-20°$. However, this may have been caused by their narrow velocity coverage, $V_{\rm LSR}=-1.6$ to 81 km s^{-1}. It should be noted that the velocities in NGC 6946 range over ± 100 km s^{-1} around the systemic velocity, namely $V_{\rm LSR}=-40$ to 160 km s^{-1}. If we compare it with our velocity field map (figure 9a), we can see that this bar is parallel to the velocity contours near the minor axis. In fact it was possible to reproduce a similar bar-like structure from our data by cutting the data outside $0<V_{\rm LSR}<80$ km s^{-1}.

(b) Mass of the Molecular Gas

We adopt the same CO-to-H_2 conversion formula used for the FCRAO 14-m telescope (Young and Scoville 1982). However, in order to obtain the conversion coefficient for our telescope, our integrated intensity at the center after convolution with the same beam as the 14-m telescope (50″ HPBW), 36.1 K km s^{-1}, was compared with the intensity obtained by Young and Scoville (1982), 46.4 K km s^{-1}. The ratio of the antenna temperatures with the 14-m and 45-m telescopes is taken to be 46.4/36.1= 1.3. Then we obtain the following expression to relate the CO intensity (K km s^{-1}) and the surface mass density:

$$\sigma_{\rm H_2}=(8\pm 4)I_{\rm CO}\cos i\ M_\odot\ {\rm pc}^{-2}\ . \tag{2a}$$

The average intensity within radius 2.2 kpc (observed area) has been obtained to be $\langle I_{\rm CO}\rangle=26.6$ K km s^{-1}. The average column density in this area is, therefore,

$$\langle\sigma_{\rm H_2}\rangle=(180\pm 90)\ M_\odot\ {\rm pc}^{-2}\ . \tag{2b}$$

The total mass of H_2 gas within 2.2 kpc is thus obtained to be

$$M({\rm H_2})(r<2.2\ {\rm kpc})=(3\pm 1.5)\times 10^9\ M_\odot\ . \tag{2c}$$

This mass is approximately 15% of the total dynamical mass in the same region, which is estimated through $M\sim(rV_{\rm rot}^2)/G\sim 2\times 10^{10}\ M_\odot$ with $r\sim 2$ pkc and $V_{\rm rot}\approx 200$ km s^{-1} (see section 4). On the other hand the H I mass in the same area is estimated as $<10^8\ M_\odot$ (Tacconi and Young 1986). This indicates that the gas in the central region is mostly in the form of molecular hydrogen, or $M({\rm H_2})/[M({\rm H_2})+M({\rm H\ I})]>97\%$. In table 2 we summarize the derived gaseous masses.

(c) "Main Disk+Nuclear Disk" Structure

Figure 3 shows the radial distribution of the integrated intensities at the observed points, where the distance from the center has been calculated by taking into account

Table 2. Gaseous masses in NGC 6946.

Gas	Region r (kpc)<	Mass ($M_\odot$)	Reference
H_2	1.5	5.0×10^8	Morris and Lo (1978)
	2.2	3.0×10^9	This paper
	12	1.1×10^{10}	Young and Scoville (1982)
H I	30	1.1×10^{10}	Tacconi and Young (1986)
	27.2	2.1×10^{10}	Rogstad and Shostak (1972)

the inclination of the disk plane. The data are fitted with the line drawn in the figure, and the intensity distribution at $r \lesssim 2$ kpc is represented by an exponential law with a scale radius of 0.93 kpc. On the other hand we know that the outer CO disk is also well represented by an exponential disk with a much larger scale radius of 4.3–4.6 kpc (Young and Scoville 1982; Tacconi and Young 1986). In table 3 we summarize the scale radii for various gaseous components when the disk is fitted with an exponential law.

Table 3. Scale radii of distributions of various components.

Component	Scale radius r_0 (kpc)	Region (kpc)	Reference
H I	14.4±0.1	$10<r<29$	Tacconi and Young (1986)
H_2	4.6±0.1	$2<r<14$	Young and Scoville (1982)
H_2	0.93±0.1	$r<2$	Present work
H I+H_2	5.6±0.1	$2<r<14$	Tacconi and Young (1986)
Hα	5.0±0.1	$2<r<12$	DeGioia-Eastwood et al. (1984)
Blue intensity	4.3±0.1	$2<r<24$	Ables (1971)
I-band	6.3±0.1	...	Elmegreen and Elmegreen (1984)
49 cm*	4.7±0.3	...	van der Kruit et al. (1977)
21 cm*	4.1±0.3	...	van der Kruit et al. (1977)

* Radio continuum.

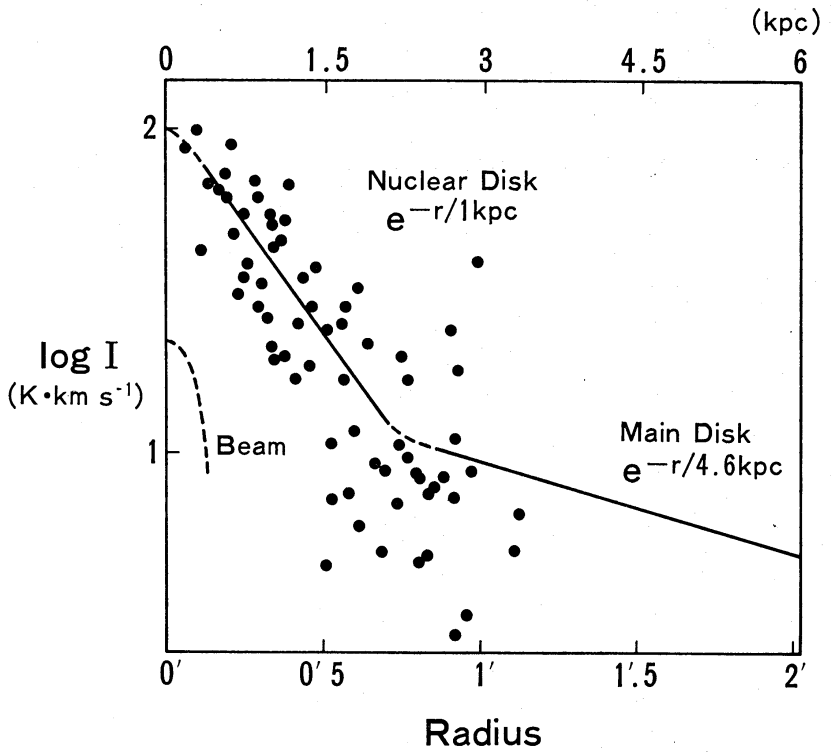

Fig. 3. Radial distribution of the integrated intensity of the CO emission. The solid line shows the exponential-law relation, $I=I_0 \exp(-r/r_0)$ fitted to the data, where $I_0=110$ K km s^{-1} and $r_0=0.93$ kpc. In the outer region of 2–14 kpc the CO distribution obeys another exponential law of $I_0=18$ K km s^{-1} and $r_0=4.6$ kpc (Young and Scoville 1982).

From these we find that the nuclear condensation of CO gas is a structure distinct from the extended main disk. We may conclude that the CO disk of NGC 6946 is composed of two distinct components: the nuclear disk and the main disk. The CO intensity distributions are represented as follows:

$$I=I_{\rm ND}\exp(-r/0.93\ {\rm kpc}) \quad \text{for} \quad r<2\ {\rm kpc\ (nuclear\ disk)} \tag{3}$$

and

$$I=I_{\rm MD}\exp(-r/4.6\ {\rm kpc}) \quad \text{for} \quad r>2\ {\rm kpc\ (main\ disk)} \tag{4}$$

with $I_{\rm ND}=110$ K km s^{-1} and $I_{\rm MD}=18$ K km s^{-1}. Figure 3 shows the radial distribution of CO intensity in NGC 6946 thus obtained.

(d) Central CO Core ?

The CO line profile of the center position $(X, Y)=(0, 0)$ has an excess at $V=V_{\rm sys}$ $(=60$ km s$^{-1})$ over the profile expected from a rotating disk. The CO line profiles on the central several points, namely at $-7''.5<X<7''.5$, $-7''.5<Y<7''.5$, have also a shoulder-like enhancement at $V\sim V_{\rm sys}$ with a velocity width of about 30 km s^{-1} (figure 1a). This excess feature is also seen in the profiles obtained by Weliachew et al. (1988) with the 30-m telescope. These shoulders can be attributed to another component located close to the galactic center which is seen within our finite beam size. Each profile at several central points is therefore an addition of the emission from the disk in rotation and the emission from antother unresolved compact "core" of molecular cloud(s) near the center. The size of the emission region is much smaller than the HPBW, or the diameter should be smaller than a few hundred parsecs. This unresolved core has an antenna temperature of 0.1 K and a line width of about 30 km s^{-1}. We can estimate the total mass of the molecular hydrogen in this core to be about $10^7\ M_\odot$.

(e) Comparison with Optical Data and the Star Formation Rate

The distribution of the optical continuum emission at 6200 Å (DeGioia-Eastwood et al. 1984) is slightly elongated in the north-south direction and approximately follows the oval distribution of the CO gas. The continuum emission in this band roughly shows the distribution of stars and therefore the overall potential is slightly elongated in the direction of the major axis of the CO oval distribution. An Hα emission map (DeGioia-Eastwood et al. 1984) shows also elongation and is correlated with the CO distribution. Hα emission may be a measure of star formation, and the correlation suggests a response of the star formation rate with the molecular gas.

In order to derive the star formation efficiency in the nuclear disk, we compare the CO intensity with the blue-light intensity (Ables 1971) in figure 4. The CO intensity is better correlated with the blue-light intensity than with that at 6200 Å or with Hα emission. In figure 5 we plot the CO and blue intensities for individual positions, where the CO observations were made. Here the blue intensity map was convolved with a 17″ Gaussian beam. From figure 5 we can derive an approximate relationship between the CO and the blue intensities,

$$I_{\rm blue}\propto I_{\rm CO}^{0.3\pm0.1} \quad \text{for} \quad r<2\ {\rm kpc}\,. \tag{5}$$

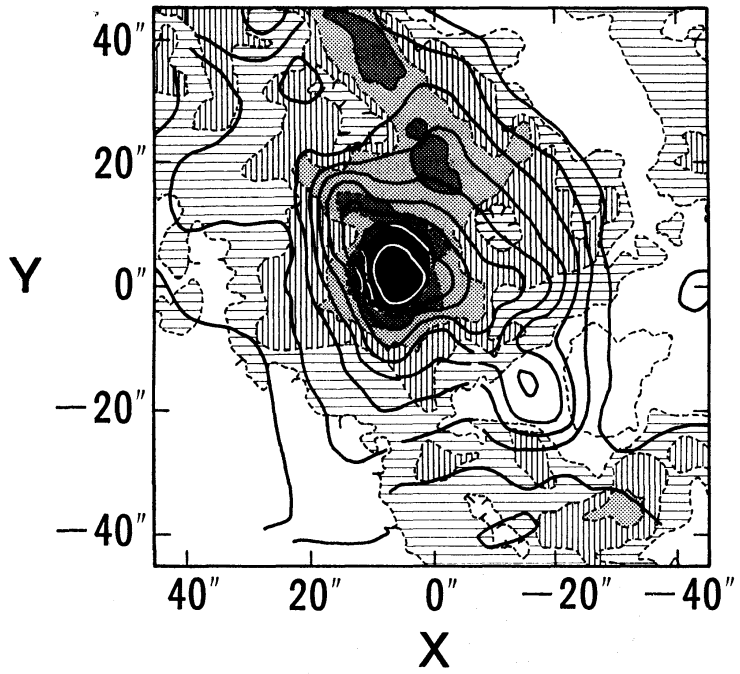

Fig. 4. Superposition of the CO intensity distribution on the blue intensity map (shaded) from Ables (1971). The blue intensity contours are 22.52, 21.66, 21.54, 21.40, and 21.18 mag arcsec^{-2}, respectively. The peak intensity is 20.01 mag arcsec^{-2}. The peak positions of both maps have been adjusted to coincide with each other.

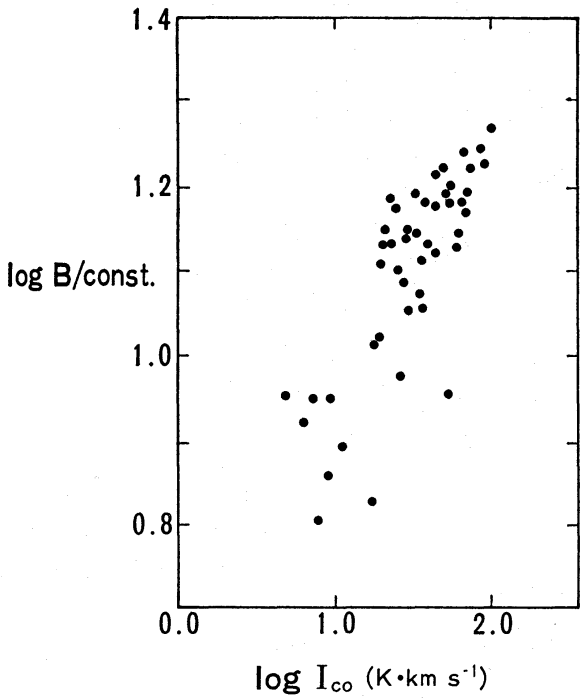

Fig. 5. Plot of the CO intensity versus blue intensity for individual observed points within $r<2$ kpc. This figure shows a power-law correlation between the CO and blue intensities.

This relation shows a smaller-power relation of the blue intensity to CO intensity, which must be compared with the first-power (linear) relation in the outer disk as obtained by Young and Scoville (1982).

This difference of the power indices in the nuclear and main disks may be attributed to several reasons: (a) The obscuration of star light in the central region is much larger than in the outer disk, so that the relation obtained here does not give a true star formation efficiency, even if it is not significantly different from the efficiency in the outer disk. (b) The conversion factor from the CO intensity to H_2 mass is different in the central region from the outer region, so that the CO intensity gives an overestimation of the H_2 mass surface density, and therefore the star formation efficiency may not be significantly different from that in the main disk. (c) The blue intensity is a real indicator of the star formation efficiency and the conversion factor of the CO intensity to the mass is correct. If this is the case, the star formation efficiency from the gas in the central region is really smaller than that in the outer region. This is consistent with the rapid accretion of gas toward the center (see section 4), and suggests a pre-starburst phase in the nuclear region.

In addition to the above relationship we note that the blue intensity has a sharper peak near the nucleus (Ables 1971) and that the CO gas has also a central core as shown in the previous subsection. Although these structures are beyond our resolution, it is possible that these two are related and a more compact, intense star forming core is present at the nucleus.

(f) Comparison with Radio Continuum Emission and Magnetic Field

NGC 6946 exhibits strong radio emission indicating a strong magnetic field and high cosmic ray density (Klein et al. 1982). Gioia and Fabbiano (1987) mapped the central region with the VLA at 6-cm wavelength and presented a map convolved to a resolution of 25″. The radio continuum distribution shows also an oval structure and resembles the CO distribution. Figure 6 compares the continuum and CO intensity distributions. Figure 7 is a plot of the CO and continuum intensities to show that the two are well correlated, for which we obtain the best-fit relation as

$$I_{6\,\mathrm{cm}} \propto I_{\mathrm{CO}}^{2.5\pm0.4} . \tag{6}$$

If the radio emission is synchrotron and an equilibrium between the energy densities of cosmic rays and magnetic field holds, we have an approximate relation between the intensity and magnetic field strength B as $I_{\mathrm{cont}} \propto B^{7/2}$. This relation and equation (6) lead to a relation between the magnetic energy density and the CO intensity:

$$\frac{B^2}{8\pi} \propto I_{\mathrm{CO}}^{1.4} . \tag{7}$$

The local relation (7) in the nuclear disk seems to be different from the linear relationship between the magnetic energy and gas density among normal disks of spiral galaxies, where the velocity dispersion is supposed to be almost constant (Sofue et al. 1986).

On the other hand it is supposed that the magnetic energy is in equilibrium with the turbulent energy of the molecular gas. Then we have a relation between the velocity dispersion and the molecular gas density as

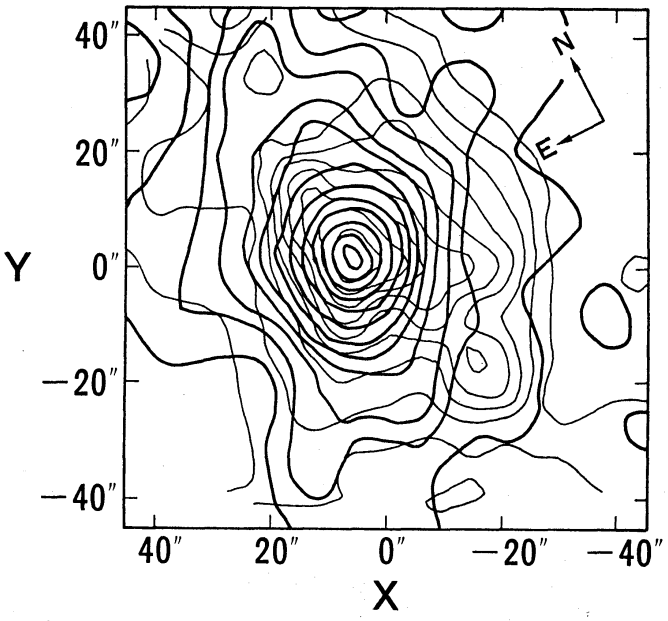

Fig. 6. Superposition of the CO (thin lines) and radio continuum (6 cm; thick lines) intensity distributions, showing a correlation between the two maps. The radio continuum map (smoothed to 25″ resolution) was taken from Gioia and Fabbiano (1987). The continuum contours are 0.4, 0.7, 1.1, 1.8, 2.6, 4.4, 7.3, 11, 15, 20, 26, and 31 mJy/beam, respectively. The peak positions have been adjusted to coincide with each other.

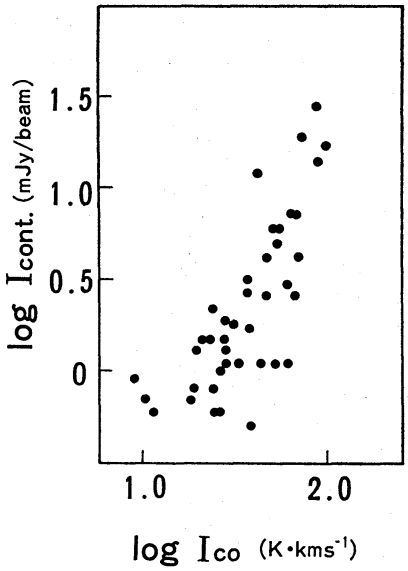

Fig. 7. Plot of the CO intensity versus the 6-cm continuum intensity, which is fitted by the relation $I_{6\,cm} \propto I_{CO}^{2.5}$.

$$\frac{B^2}{8\pi} \sim \frac{1}{2}\rho_{gas}\sigma_v^2 \propto \left(\frac{I_{CO}}{L}\right)\sigma_v^2 , \qquad (8)$$

where σ_v is the velocity dispersion, ρ_{gas} the gas density, and L is the thickness of the gas layer. Finally we obtain a relation as

$$\frac{\sigma_v^2}{L} \propto I_{CO}^{0.4} \propto \exp(r/2.3 \text{ kpc}) . \quad (9)$$

This relation implies that either the velocity dispersion decreases or the disk thickness increases with increasing radius.

4. Kinematics and Dynamics

(a) Kinematics

Using the observed data we obtain several diagrams showing the kinematics in the central region of NGC 6946. Figure 8 shows the position-velocity diagrams along the major and minor axes. From the diagram along the major axis we derive the systemic velocity as V_{sys}(LSR)=60 km s^{-1}, on the assumption that the maximum peak velocities are symmetric with respect to the systemic center. This value is consistent with the one derived from the H I observations (Tacconi and Young 1986) and is used throughout this paper.

Figure 9 shows the peak- and mean-velocity fields. The isovelocity contours have a systematic inclination relative to the minor axis (Y) of about 10°, while the velocity field near the major axis (X) is consistent with circular rotation. Here we took the major axis at a position angle 62° from the north.

Figure 10 shows equal-velocity intensity maps for 12 velocity channels, where the distribution of the CO intensity integrated in each 20-km s^{-1} interval is displayed in the X-Y coordinates. The fact that the intensity peak appears always on the X axis in any velocity range indicates that the major axis of the CO distribution coincides well with that obtained from the H I observation of the outer region.

Figure 11 shows the rotation curve obtained from the velocity structure along the major axis corrected for the inclination of the galaxy plane. The CO rotation curve can be smoothly combined with the outer rotation curve as derived from the H I observations by Tacconi and Young (1986) (figure 11b). The whole curve shows a flat rotation toward the central region as close as 500 pc of the nucleus, while the rotation velocity has a steep gradient at $r<500$ pc.

(b) Discrepancy of the CO and Optical Velocities

Beckman et al. (1986) derived velocity curves in the central region from the Hα emission line, which indicates the motion of H II gas along four axes at PA=67°, 157°, 22°, and 292°. An optically determined velocity curve along the major axis is flat at a constant value of 50 km s^{-1}, while velocities along the axis at PA=157° (minor axis) reach 100 km s^{-1}. The velocities along the axis of PA=17° are smaller than the systemic velocity, or $V-V_{sys}<0$ in the northeastern part, and $V-V_{sys}>0$ in the southwestern part. However, the sign of the value of $V-V_{sys}$ in our CO observations is the inverse of the tendency in the optical velocities.

The discrepancy between the optical and CO data may be attributed to the fact that we are looking at different places and motions in the two gaseous components, H II and molecular gases. A similar discrepancy in the optical and CO data was found also in M82 (Nakai et al. 1987).

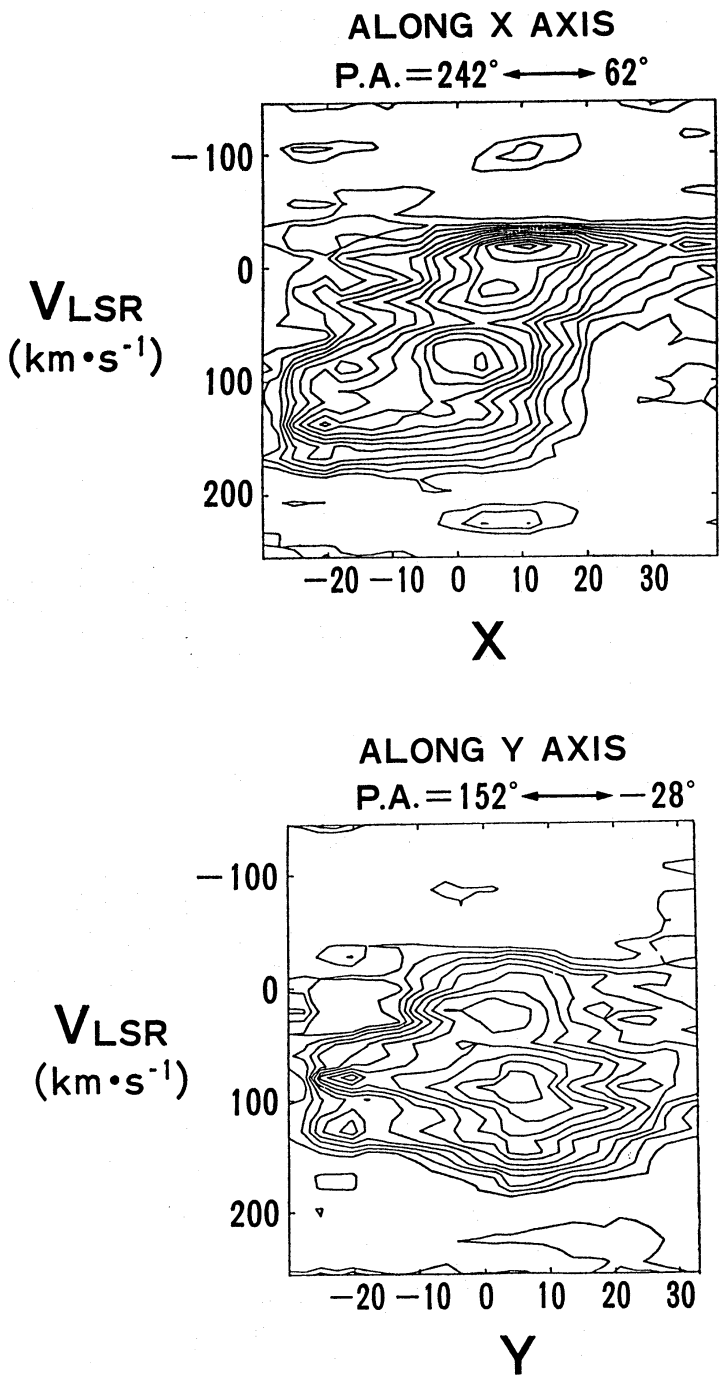

Fig. 8. Position-velocity maps of the CO line along the major (X) and minor (Y) axes.

Beckman et al. (1986) assigned the Hα velocities to a radial motion of the H II gas within the disk. They suggest that the radial motion may be an expansion caused by an energy input by 15,000 O5 stars surrounding the nucleus. However, considering the trailing rotation sense of NGC 6946, the excess of the optical velocity seems more convincingly attributed either to a contraction or to a noncoplanar motion, e.g., a motion perpendicular to the disk plane.

(c) Velocity Field and Noncircular Motion

In figure 9c we superpose the CO velocity field (figure 9a) on the H I velocity field obtained by Tacconi and Young (1986). The position angle of the CO contour alignment near the minor axis in the nuclear region is significantly inclined from the one

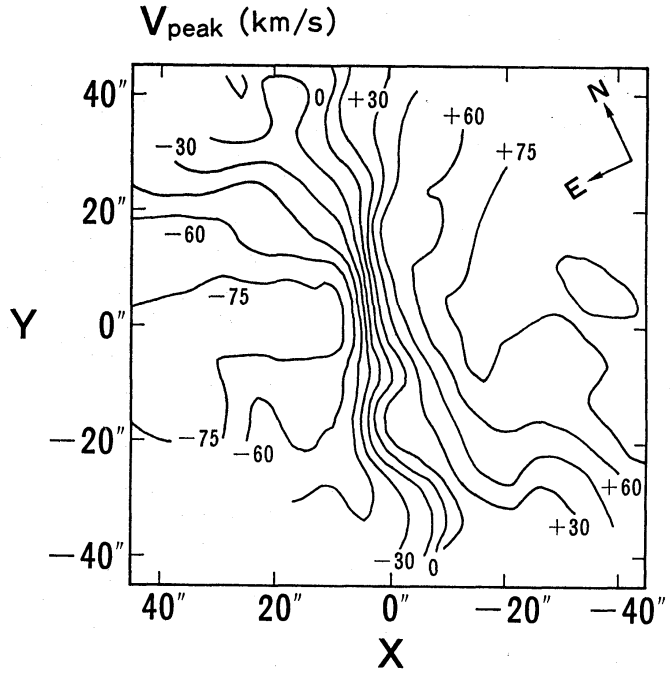

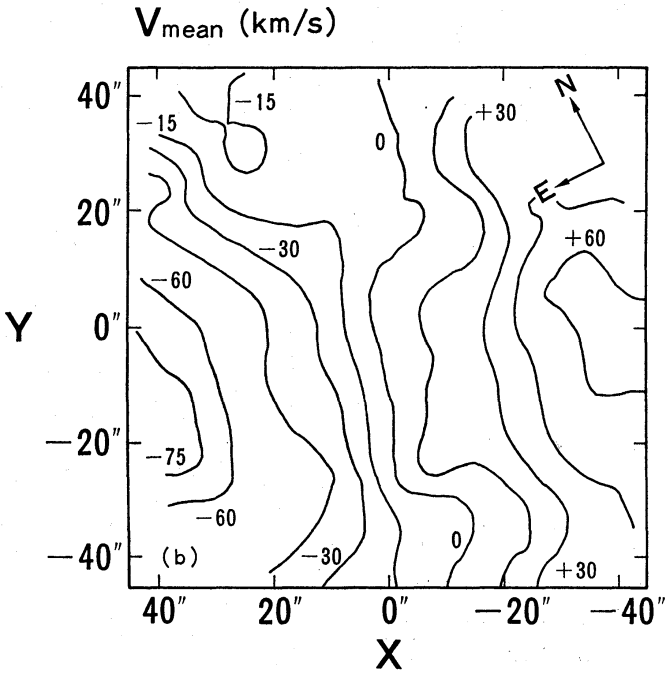

Figs. 9a and b. See the legend on the next page.

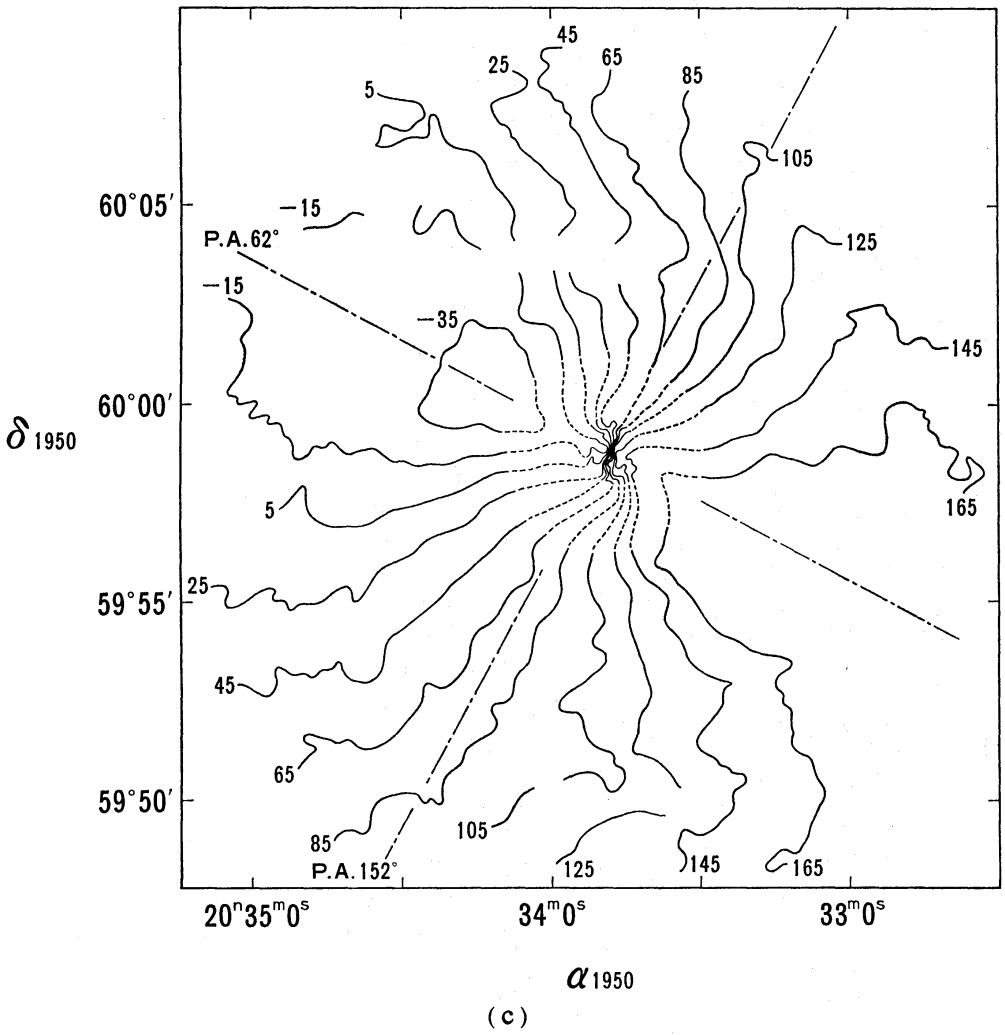

Fig. 9. (a), (b) Peak- and mean-velocity fields of the CO line emission. Velocity values for the contours are in intervals of 15 km s^{-1} relative to the systemic velocity ($V_{LSR}-V_{sys}$). Note that the isovelocity contours near the minor axis incline about 9° from the Y axis. (c) A map of CO peak velocity field combined with the outer H I mean velocity field (Tacconi and Young 1986). Velocity values for the contours are V_{LSR} in intervals of 20 km s^{-1}. The dash-dotted straight lines show the major and minor axes at position angle 62° and 152°, respectively.

extrapolated from the outer H I field. The variation in the kinematical position angle between the inner and outer disks has been noted also by Tacconi and Young (1986). Such a variation suggests two possibilities: (1) Since the apparent CO velocity is not independent of the mass distribution of molecular gas because of the finite beam size, the intensity deficiency in the northwestern and southeastern regions may cause an apparent inclination of the velocity contours. (2) The influence of the gas distribution is small, and the asymmetry reflects real velocities.

The first possibility may be not the case, or at least not significant, because the velocity field obtained from peak velocities (figure 9a) shows the same amount of inclination as that obtained from mean velocities (figure 9b). If an asymmetric gas distribution was the cause, the mean-velocity field must have even larger inclination than

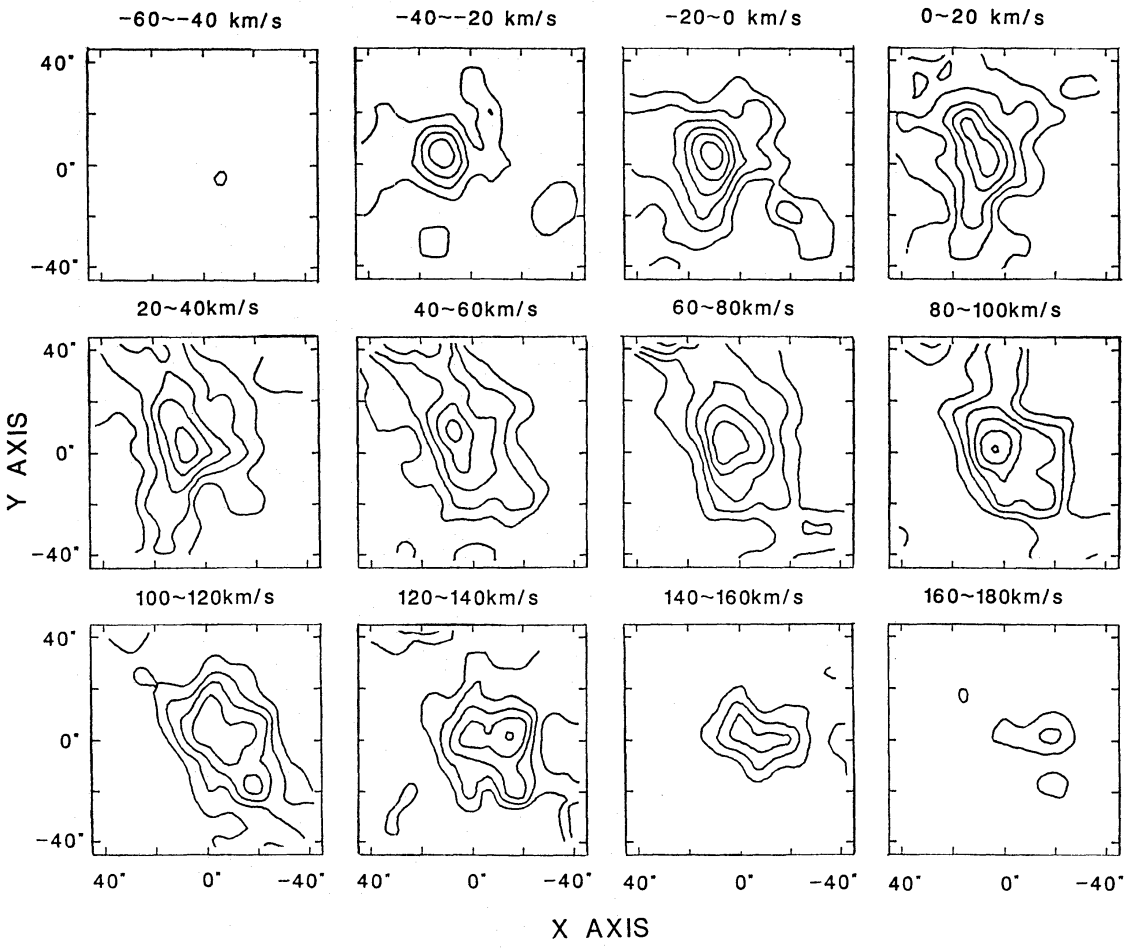

Fig. 10. CO integrated intensity map for 12 velocity channels. The contours are in intervals of 10 K km s^{-1} and the lowest level is 10 K km s^{-1}. Velocity values are relative to LSR. The fact that intensity peak positions lie always on the *X*-axis shows that the position angle of the major axis is about 62° and excludes the possibility of the warping of this galaxy.

in the symmetric case. So we here consider the second possibility more seriously.

The inclination of the velocity field may be caused by the following two possible effects: (A) NGC 6946 is a warped galaxy, or (B) the galaxy has a noncircular motion in the nuclear region. If possibility A was the case, the major axis derived from the velocity field must be also inclined from that of the outer disk. However, as seen from the equal-velocity maps (figure 10) the intensity peaks in all channels lie on the major axis derived from the H I data. This fact seems to deny possibility A. We therefore conclude that the asymmetric velocity field in figure 9 is caused by a noncircular motion.

Considering the inclination and trailing-sense rotation, the noncircular motion is most convincingly attributed to a radial contraction (inflow). The fact that the peak- and mean-velocity fields show the same noncircular velocities indicates that a considerable portion or all of the gas is inflowing. This implies that the motion is in the disk plane. It is difficult to argue that the gas in or near the disk is expanding perpendicu-

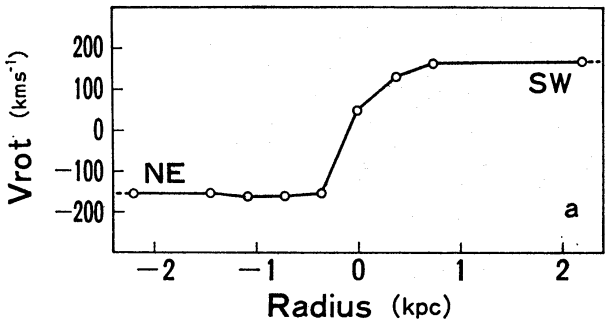

(a)

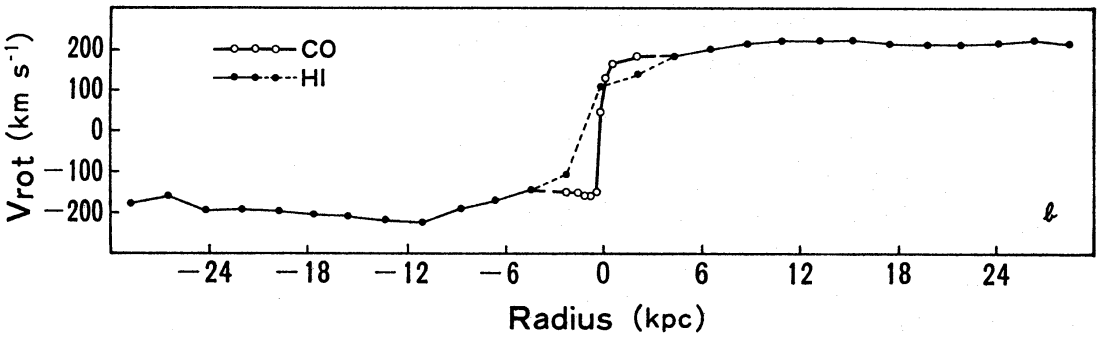

(b)

Fig. 11. (a) CO rotation velocities corrected for the inclination of the galaxy measured along the X (major)-axis. Adopted systemic velocity is V_{sys} (LSR)=60 km s^{-1}. These velocities are measured at the line edge. (b) CO peak rotation velocities combined with the H I mean rotation velocities (Tacconi and Young 1986). The adopted systemic velocity V_{sys} (LSR)=60 km s^{-1}. The rotation velocity of the disk is almost constant.

larly to the galactic plane, because the motion then must be symmetric with respect to the disk and no asymmetric shift (inclination) of the velocity field is expected. A bipolar outflow in the halo may cause an asymmetric shift of the wings of the velocity profiles. However, it seems difficult to cause a shift of the profile peaks as observed here.

(d) Bar-Shocked Model for the Noncircular Motion and Accretion

We may conclude that the most reasonable explanation of the CO gas motion in the nuclear region is a radial inward motion within the galactic plane. The radial velocity V_r of the inward motion (superposed on the pure rotation) can be estimated as V_r=40 km s^{-1} ar r=30″ on the minor axis. If this inward motion is a pure inflow, the molecular gas within 1.5-kpc radius falls into the region very close to the nucleus in $\sim 10^8$ yr, or the accretion rate is as high as $\sim 70\ M_\odot$ yr^{-1}. Such a high accretion rate must cause various activities in the nucleus, although we see no definite sign of a star burst, in NGC 6946.

On the other hand the observed noncircular (inflow) motion can be well explained by a theoretical model of gas motion in a barred spiral galaxy (e.g., Sørensen et al. 1976; Roberts et al. 1979; Prendergast 1983; Noguchi 1988). Based on the bar-shocked model, Roberts et al. (1979) have calculated the motion of gas clouds. Using

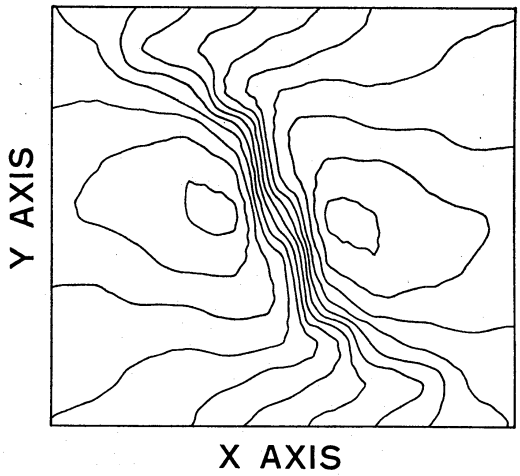

Fig. 12. A model velocity field for the central region of NGC 6946 as calculated based on the barred-shocked model of Roberts et al. (1979) for the parameters in table 1.

their result we produced a velocity field, where we took the parameters given in table 1. The result is shown in figure 12, and we find that the model reasonably agrees with the observed velocity field in figure 9a. The observed radial velocity V_r=40 km s^{-1} is of the same order as the theoretical value (50–150 km s^{-1}) predicted by Roberts et al. (1979). In this case the cause for the skewing of the isovelocity contours is primarily the elliptical trajectories of the gas clouds rather than by a pure inflow toward the nucleus. It is also pointed out by Combes (1988) that an oval distortion of the mass distribution may play the same role as a bar, and an accretion of gas is expected in the same manner as in the barred spiral galaxy.

An alternative model for the accretion of gas without a bar has been proposed by Fukunaga (1983). He showed that the viscosity via collisions of clouds even in circular orbits causes a loss of kinetic energy and a transfer of angular momentum, and results in an accretion of gas toward the center. However, this model without assuming a bar seems to be difficult to account for the observed high inward velocity.

5. Summary

The results of our observations and discussion are summarized as follows:

(i) The CO distribution has a strong central concentration and slight elongation in the direction of PA=0–30°.

(ii) The average column density and total mass of H_2 gas within the radius 2.2 kpc are estimated as 180 $M_\odot$ pc^{-2} and 3×10^9 $M_\odot$, respectively. This comprises 15% of the total (dynamical) mass of the region.

(iii) The CO disk of NGC 6946 is composed of two distinct exponential disks: the nuclear disk and the main disk, whose intensity distributions are given by equations (3) and (4).

(iv) Central CO profiles imply that there exists an unresolved compact core of molecular cloud(s) besides the disk components. The mass of this core is approximately 10^7 $M_\odot$.

(v) The blue star-light intensity is related to the CO intensity as equation (5), which indicates either an extremely high obscuration of star light in the nuclear disk or low star formation efficiency compared with that in the disk.

(vi) The radio continuum intensity is related to the CO intensity as equation (6), suggesting a higher strength of magnetic field and/or a high rate of cosmic ray acceleration in the nuclear region.

(vii) The rotation curve shows a flat rotation even in the central region as close 500 pc of the nucleus, while it has a steep gradient at $r<500$ pc.

(viii) The CO velocity field has a different tendency from that of the Hα velocity field. This may be attributed to the fact that we are looking at different places and motions in the H II and H_2 gaseous components.

(ix) The most reasonable kinematic model of the CO motion in the nuclear region is a contracting disk in rotation with the radial inflow velocity of about 40 km s^{-1} at $r=1.5$ kpc. A bar-shocked model agrees with the observed velocity field.

(x) Accretion of the molecular gas to the central narrow region may be explained either by this bar-shocked model or by the mechanism that the viscosity during cloud collisions causes loss of kinetic energy and angular momentum (Fukunaga 1983; Noguchi 1988).

We wish to thank K. Shinjo for his help in the observations and reduction in the initial stage of this project. We also thank the Ministry of Education, Science, and Culture for the financial support under Grant No. 61460009 (Y. Sofue).

References

Ables, H. D. 1971, *Publ. U. S. Naval Obs., Ser. 2*, **20**, Part 4.
Arp, H. 1966, *Astrophys. J. Suppl.*, **14**, 1.
Ball, R., Sargent, A. I., Scoville, N. Z., Lo, K. Y., and Scott, S. L. 1985, *Astrophys. J. Letters*, **298**, L21.
Beckman, J. E., Mũoz Tuñon, C., Battaner, E., Prieto, M., and Sanchez Saavedra, M. L. 1986, *Astron. Astrophys.*, **161**, 55.
Combes, F. 1988, in *Galactic and Extragalactic Star Formation*, ed. R. E. Pudritz and M. Fich (Kluwer Academic Publishers, Dordrecht), p. 475.
Condon, J. J., Condon, M. A., Gisler, G., and Puschell, J. J. 1982, *Astrophys. J.*, **252**, 102.
DeGioia-Eastwood, K., Grasdalen, G. L., Strom, S. E., and Strom, K. M. 1984, *Astrophys. J.*, **278**, 564.
Elmegreen, D. M., and Elmegreen, B. G. 1984, *Astrophys. J. Suppl.*, **54**, 127.
Fukunaga, M. 1983, *Publ. Astron. Soc. Japan*, **35**, 173.
Gioia, I. M., and Fabbiano, G. 1987, *Astrophys. J. Suppl.*, **63**, 771.
Hodge, P. W. 1969, *Astrophys. J. Suppl.*, **18**, 73.
Klein, U., Beck, R., Buczilowski, U. R., and Wielebinski, R. 1982, *Astron. Astrophys.*, **108**, 176.
Lebofsky, M. J., and Rieke, G. H. 1979, *Astrophys. J.*, **229**, 111.
Lo, K. Y., Phillips, T. G., Knapp, G. R., and Wootten, H. A. 1980, *Bull. American Astron. Soc.*, **12**, 859.
Morris, M., and Lo, K. Y. 1978, *Astrophys. J.*, **223**, 803.
Nakai, N., Hayashi, M., Handa, T., Sofue, Y., Hasegawa, T., and Sasaki, M. 1987, *Publ. Astron. Soc. Japan*, **39**, 685.
Noguchi, M. 1988, *Astron. Astrophys.*, **203**, 259.
Prendergast, K. H. 1983, in *Internal Kinematics and Dynamics of Galaxies, IAU Symp. No. 100*, ed. E.

Athanassoula (D. Reidel Publishing Company, Dordrecht), p. 215.
Rickard, L. J., and Harvey, P. M. 1984, *Astron. J.*, **89**, 1520.
Rickard, L. J., and Palmer, P. 1981, *Astron. Astrophys.*, **102**, L13.
Roberts, W. W., Jr., Huntley, J. M., and van Albada, G. D. 1979, *Astrophys. J.*, **233**, 67.
Rogstad, D. H., and Shostak, G. S. 1972, *Astrophys. J.*, **176**, 315 (RS 1972).
Rogstad, D. H., Shostak, G. S., and Rots, A. H. 1973, *Astron. Astrophys.*, **22**, 111 (RSR 1973).
Sandage, A., and Tammann, G. A. 1974, *Astrophys. J.*, **194**, 559.
Sandage, A., and Tammann, G. A. 1981, *A Revised Shapley–Ames Catalog of Bright Galaxies* (Carnegie Institution of Washington, Washington, D. C.).
Sofue, Y., Fujimoto, M., and Wielebinski, R. 1986, *Ann. Rev. Astron. Astrophys.*, **24**, 459.
Sørensen, S.-A., Matsuda, T., Fujimoto, M. 1976, *Astrophys. Space Sci.*, **43**, 491.
Tacconi, L. J., and Young, J. S. 1986, *Astrophys. J.*, **308**, 600.
van den Bergh, S. 1960, *Astrophys. J.*, **131**, 215.
van der Kruit, P. C., Allen, R. J., and Rots, A. H. 1977, *Astron. Astrophys.*, **55**, 421.
Weliachew, L., Casoli, F., and Combes, F. 1988, *Astron. Astrophys.*, **199**, 29.
Young, J. S., and Sanders, D. B. 1986, *Astrophys. J.*, **302**, 680.
Young, J. S., and Scoville, N. 1982, *Astrophys. J.*, **258**, 467.